Theoretical model of the nonlinear resonant interaction of whistler-mode waves and field-aligned electrons.

A. V. Artemyev,[1, a)] A. I. Neishtadt,[2, b)] J. M. Albert,[3] L. Gan,[4] W. Li,[4] and Q. Ma[4]
[1)] *Institute of Geophysics and Planetary Physics, University of California, Los Angeles, USA.*
[2)] *Department of Mathematical Sciences, Loughborough University, Loughborough LE11 3TU, United Kingdom.*
[3)] *Air Force Research Laboratory, Kirtland Air Force Base, Albuquerque, NM USA.*
[4)] *Center for Space Physics, Boston University, Boston, MA USA.*

(Dated: 1 January 2021)

The nonlinear resonant interaction of intense whistler-mode waves and energetic electrons in the Earth's radiation belts is traditionally described by theoretical models based on the consideration of slow-fast resonant systems. Such models reduce the electron dynamics around the resonance to the single pendulum equation, that provides solutions for the electron nonlinear scattering (phase bunching) and phase trapping. Applicability of this approach is limited to not-too-small electron pitch-angles (i.e., sufficiently large electron magnetic moments), whereas model predictions contradict to the test particle results for small pitch-angle electrons. This study is focused on such field-aligned (small pitch-angle) electron resonances. We show that the nonlinear scattering can be described by the slow-fast Hamiltonian system with the separatrix crossing. For the first cyclotron resonance, this scattering results in the electron pitch-angle increase, contrast to the pitch-angle decrease predicted by the pendulum equation. We derive the threshold value of the magnetic moment of the transition to a new regime of the nonlinear resonant scattering. For field-aligned electrons the proposed model provides the magnitude of magnetic moment changes due to the nonlinear scattering. Together with existing models for not-too-small pitch-angles, this model completes the theory of the nonlinear resonant electron interaction with intense whistler-mode waves.

I. INTRODUCTION

The wave-particle resonant interaction is the key process for energy exchange between different particle populations in collisionless plasma[24]. Particle scattering by waves is responsible for losses in magnetic traps[76], e.g. in Earth's radiation belts[8,39] where whistler-mode chorus and hiss waves together with electromagnetic ion cyclotron waves control electron precipitations into Earth's atmosphere[46,48,73]. The basic concept describing such scattering is the quasi-linear theory[20,77] that assumes electron resonant interaction with a broad-band spectrum of low coherent, low amplitude waves[64]. In an inhomogeneous ambient magnetic field the requirement for a low coherence is significantly relaxed[33,45], and electron scattering by the monochromatic low amplitude waves can be described by the quasi-linear diffusion[4,5]. However, effects of electron resonances with intense waves, e.g. phase trapping and nonlinear scattering (phase bunching)[34,35,58,59], are well beyond the quasi-linear theory and require a separate consideration[7,12,63,66].

Although oblique whistler-mode waves represent a significant fraction of whistlers in the Earth's radiation belts[10], the most intense are field-aligned whistlers[74,78,81] (e.g., lower band chorus waves with the wave frequency ω below a half of the electron gyrofrequency, Ω_{ce}), which often resonate with electrons nonlinearly[79]. There is only the first cyclotron resonance available for field-aligned whistler-mode waves interacting with electrons: $\gamma\omega - kc\sqrt{\gamma^2-1}\cos\alpha = \Omega_{ce}$ (k is the wavevector, α is an electron pitch-angle, and γ is an electron Lorentz factor). The phase trapping for this resonance results in electron acceleration with the electron pitch-angle increase for energetic particles (with the $\gamma < \Omega_{ce}/\omega$) and with the electron pitch-angle decrease for ultra-relativistic particles (with $\gamma > \Omega_{ce}/\omega$), see Refs. 23, 62, and 69. The nonlinear scattering (phase bunching) results in decrease of electron energy and pitch-angle[3,14]. Although effects of realistic wave frequency drift[18,19,32,38,42] and wave amplitude modulation[25,31,71,72] alter the electron nonlinear resonant interaction, the basic concept remains the same: trapping results in electron transport away from the loss-cone and nonlinear scattering results in electron transport toward the loss-cone. A competition of these two nonlinear processes determines electron acceleration and losses.

The theory of nonlinear electron resonances with whistler-mode waves is based on individual orbit analysis, that reduces the electron motion equation to the pendulum equation with torque[2,15,56,58,65]. Such analysis describes well both phase trapping and nonlinear scattering effects and provides typical amplitudes of energy and pitch-angle changes, $\Delta\gamma$ and $\Delta\alpha$. The basic idea behind this analysis is the separation of time-scales of fast variations of resonant phase (the inverse time scale is $\sim \dot{\phi} \sim \omega$) and slow variations of the ambient mag-

[a)] Also at Space Research Institute, RAS, Moscow, Russia; Author to whom correspondence should be addressed; Electronic mail: aartemyev@igpp.ucla.edu
[b)] Also at Space Research Institute, RAS, Moscow, Russia

netic fields along electron trajectories (the inverse time-scale is $\sim c\sqrt{1-\gamma^{-2}}/R \ll \omega$, R is a typical inhomogeneity scale). This separation provides a single small parameter $c/R\omega \sim 1/kR \ll 1$. For the nonlinear wave-particle interaction this parameter is about the ratio of a wave amplitude B_w and ambient magnetic field magnitude B_0, i.e. a wave force $\sim B_w/k$ can compete with a mirror force $\sim B_0/R$ and temporally trap electrons into the resonance[2,35,67]. However, this theoretical concept is invalid for systems with the second small parameter, e.g. for very small pitch-angle (almost field-aligned) electrons. This effect has been found in Ref. 47: the resonant interaction cannot result in decrease of electron pitch-angles below zero, and for sufficiently small pitch-angles such interaction would increase pitch-angles. Therefore, the nonlinear scattering model, predicting $\Delta\alpha < 0$, meets difficulties in describing small pitch-angle electron resonances (see discussion in Refs. 25 and 40). Test particle simulations show that $\Delta\alpha$ due to nonlinear scattering becomes positive for sufficiently small initial α (such electron *repulsion* from the loss-cone results in effective *electron trapping around loss-cone*[40]). The similar effect of the reversing of pitch-angle scattering around the loss-cone is observed for the electron resonant interaction with electromagnetic ion cyclotron waves (see Refs. 27, 28, and 41). So, the actual question is: can the theoretical model of the nonlinear wave-particle interaction be modified to account for such electron *repulsion* from the loss-cone? We address this question below.

II. BASIC EQUATIONS

We start with the Hamiltonian of a relativistic electron (m_e is the rest mass, $-e$ is the charge, energy is comparable to $m_e c^2$ where c is the speed of light) describing two pairs of conjugate variables: the field-aligned coordinate and momentum $(s, p_\parallel)$, gyrophase ψ and momentum $I_x = c\mu/e$ where μ is the classical magnetic moment. In presence of a field-aligned whistler-mode wave, this Hamiltonian can be written as (see, e.g., Refs. 7 and 75):

$$H = m_e c^2 \gamma + U_w\left(s, I_x\right)\sin\left(\phi+\psi\right)$$
$$\gamma = \sqrt{1+\frac{p_\parallel^2}{m_e^2 c^2}+\frac{2I_x\Omega_{ce}}{m_e c^2}} \qquad (1)$$

where $\Omega_{ce} = eB_0/m_e c$ is the electron gyrofrequency ($B_0(s)$ is the background magnetic field given by, e.g., reduced dipole model[15]), $U_w = \sqrt{2I_x\Omega_{ce}m_e}eB_w/\gamma m_e c k$ with B_w the wave amplitude. The wave number $k(\omega, s)$ is given by the cold plasma dispersion[68] for a constant wave frequency ω (i.e., $\partial\phi/\partial s = k$, $\partial\phi/\partial t = -\omega$). Hamiltonian equations for (1) are

$$\dot{s} = \frac{p_\parallel}{m_e\gamma}+\frac{\partial U_w}{\partial p_\parallel}\sin\left(\phi+\psi\right)$$
$$\dot{p}_\parallel = -\frac{I_x}{\gamma}\frac{\partial\Omega_{ce}}{\partial s}-kU_w\cos\left(\phi+\psi\right)-\frac{\partial U_w}{\partial s}\sin\left(\phi+\psi\right)$$
$$\dot{\psi} = \frac{\Omega_{ce}}{\gamma}+\frac{\partial U_w}{\partial I_x}\sin\left(\phi+\psi\right) \qquad (2)$$
$$\dot{I}_x = -U_w\cos\left(\phi+\psi\right)$$

where $\dot{\phi} = k\dot{s}-\omega$. Equations (2) show that in absence of wave ($U_w = 0$) and for I_x of the order of $p_\parallel^2/m_e\Omega_{ce}$ (for not too small pitch-angles), phases ϕ and ψ change with the rate $\sim\Omega_{ce}$ (we consider whistler-mode waves with ω of the order of Ω_{ce}), whereas $(s, p_\parallel)$ change with the rate $(p_\parallel/\gamma)\partial\Omega_{ce}/\partial s \sim c/R$ where R is a spatial scale of B_0 gradient (for the Earth radiation belts $R \approx R_E L$, $R_E \approx 6380$ km and L is the distance from the Earth in R_E). Comparing these rates, we obtain $c/R\Omega_{ce} \ll 1$, i.e., ϕ and ψ change much faster than $(s, p_\parallel)$ do. For intense whistler waves in the radiation belts $B_w/B_0 \geq c/R\Omega_{ce}$ despite that $B_w/B_0 \ll 1$ (see Ref. 81). Therefore, $\sim U_w$ term in Eqs. (2) does not modify the rates of ϕ, ψ and $(s, p_\parallel)$ change: phases are fast variables and field-aligned coordinate, momentum are slow variables. Hamiltonian (1) with such time-scale separation is studied both numerically and analytically[2,14,65,72]. Figure 1(a) shows several fragments of electron trajectories around the resonance $\dot{\phi}+\dot{\psi} = 0$ for this Hamiltonian. Resonant electrons can be either trapped (and accelerated) by the wave or scattered (with energy decrease). Trapping increases I_x (and increases electron equatorial pitch-angle α_{eq}; $I_x = m_e c^2\left(\gamma^2-1\right)\sin^2\alpha_{eq}/2\Omega_{ce}(0)$), whereas nonlinear scattering decreases I_x and α_{eq}. Amplitudes of energy and I_x (or pitch-angle) changes for such trapping and scattering are well described by analytical equations[3,13,75].

For electron nonlinear scattering, the amplitude of I_x changes is about $\sim\sqrt{B_w/B_0}$ (see details in, e.g., Refs. 7, 12, and 55 and references therein). However, if I_x is sufficiently small (i.e., for field-aligned electrons), these changes can be larger than the initial I_x. This would break the theory, because I_x is positively defined variable that cannot become negative. Figure 1(b) shows several fragments of field-aligned electron trajectories: there are positive I_x changes due to nonlinear scattering (compare with Fig. 1(a)). Thus, a new model should be developed to describe this nonlinear scattering for small $I_x \leq \sqrt{B_w/B_0}$.

Let us introduce new phase φ and conjugate momentum I through the generating function $W = \left(\int k(\tilde{s})d\tilde{s}-\omega t+\psi\right)I+sP$:

$$H_I = -\omega I+m_e c^2\gamma+U_w\sin\varphi$$
$$\gamma = \sqrt{1+\frac{\left(P+kI\right)^2}{m_e^2 c^2}+\frac{2I\Omega_{ce}}{m_e c^2}} \qquad (3)$$

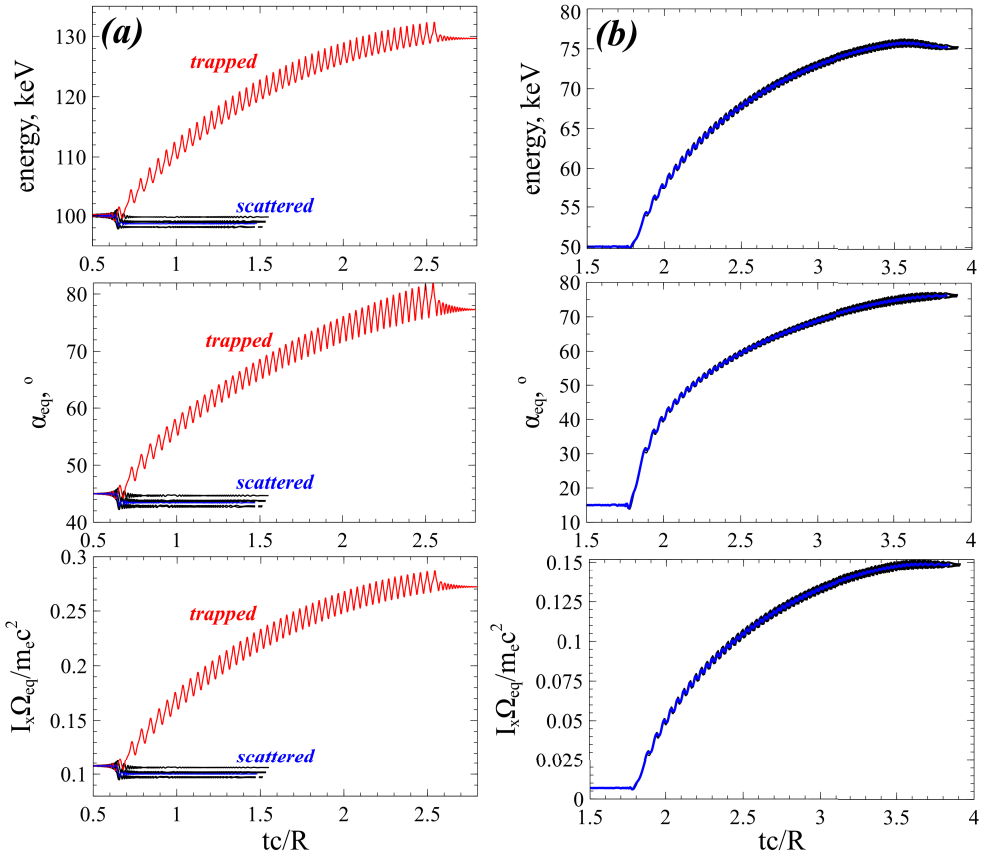

FIG. 1: Changes of electron energy, pitch-angle, and I_x ($\Omega_{eq} = \Omega_{ce}(0)$ is the electron equatorial gyrofrequency) due to nonlinear scattering (black; blue shows averaged energy of scattered particles) and trapping (red). Left and right columns show results for 45° and 5° initial equatorial pitch-angles. The time interval of one resonant interaction is shown. For these trajectories we consider the curvature-free dipole magnetic field[15] with the radial distance from the Earth $R = 6R_E$ (i.e., $L = 6$). The wave frequency is $0.35\Omega_{eq}$, and plasma frequency equals to $6\Omega_{eq}$. To evaluate the wave number k we use the cold plasma dispersion of whistler-mode waves[68]. Wave amplitude is 500 pT, i.e. this is an intense wave[17,74,78,79]. The distribution of the wave amplitude along magnetic field lines, $B_w(s)$, is modeled by function $\tanh((\lambda/\delta\lambda_1)^2)\exp(-(\lambda/\delta\lambda_2)^2)$ with λ being the magnetic latitude ($ds = Rd\lambda\sqrt{1+\sin^2\lambda}\cos\lambda$) and $\delta\lambda_1 = 2°$, $\delta\lambda_2 = 20°$. This function fits the observed whistler-mode wave intensity distribution[1]. To simplify the simulations, we consider waves only in one hemisphere, $B_w = 0$ for $s < 0$, and thus there is only one resonance within one bounce period. Waves are moving away from the equatorial plane, $s = 0$, to large s, i.e. only $k > 0$ are included.

Hamiltonian (3) does not depend on time, i.e. H_I = const and $m_e c^2\gamma - \omega I$ is the integral of motion. Far from the resonance $\dot{\varphi} = \partial H_I/\partial I = 0$, particles move in 2D surface formed by intersection of $H_I(s, P, I)$ = const and I = const. The standard procedure suggests expansion of Hamiltonian (3) around the resonance $I = I_{res}$ defined by $\partial H_I/\partial I = 0$. However, for small momentum I such an approach is not applicable. To follow an alternative approach, we start with the expansion for small I and then consider the resonance.

III. EXPANSION AROUND SMALL I

Let us consider Hamiltonian (3) for small kI values:

$$H_I \approx \left(\frac{\Omega_{ce} + kP/m_e}{\gamma_0} - \omega\right) I + \frac{K^2 I^2}{2m_e} + m_e c^2\gamma_0 + \sqrt{\frac{2I\Omega_{ce}}{m_e}}\frac{eB_w}{ck\gamma_0}\sin\varphi \qquad (4)$$

where

$$K^2 = m_e^2 c^2 \left.\frac{\partial^2\gamma}{\partial I^2}\right|_{I=0} = \frac{1}{\gamma_0^3}\left(k^2 - 2\frac{kP\Omega_{ce}}{m_e c^2} - \frac{\Omega_{ce}^2}{c^2}\right) \qquad (5)$$

and $\gamma_0 = \sqrt{1 + (P/m_e c)^2}$. Note Eq. (4) shows that $H_I \approx m_e c^2\gamma_0 + O(I)$ is the integral of motion. We rewrite

Hamiltonian (4) as

$$H_I = \Lambda + \frac{1}{2m_e}K^2\left(I-I_R\right)^2 + \sqrt{\frac{2I\Omega_{ce}}{m_e}}\frac{eB_w}{ck\gamma_0}\sin\varphi$$
$$\Lambda = m_e c^2\gamma_0 - \frac{m_e}{2K^2}\left(\omega - \frac{\Omega_{ce}+kP/m_e}{\gamma_0}\right)^2$$
$$I_R = \frac{m_e}{K^2}\left(\omega - \frac{\Omega_{ce}+kP/m_e}{\gamma_0}\right) \quad (6)$$

where $I_R = I_{res}$ is the resonant momentum, because $\partial H_I/\partial I = 0$ has a solution $I = I_R$. The Hamiltonian equations for I and φ are

$$\dot{I} = -\sqrt{2I\Omega_{ce}m_e}\frac{B_w\Omega_{ce}}{B_0 k\gamma_0}\cos\varphi \quad (7)$$
$$\dot{\varphi} = \frac{1}{m_e}K^2\left(I-I_R\right) + \sqrt{\frac{\Omega_{ce}m_e}{2I}}\frac{B_w\Omega_{ce}}{B_0 k\gamma_0}\sin\varphi$$

where coefficients depend on slowly changing (s, P). Let us introduce a small parameter

$$\varepsilon = \frac{eB_w}{m_e c^2 k_{eq}}$$

and functions

$$u = \frac{k_{eq}}{k}\sqrt{\frac{\Omega_{ce}}{\Omega_{eq}}}\frac{1}{w\gamma_0}, \quad w = \frac{K^2c^2}{\Omega_{eq}^2}$$

with $\Omega_{eq} = \Omega_{ce}(0)$, $k_{eq} = k(0)$. Then we introduce new variable $Y = I\Omega_{eq}/m_e c^2\varepsilon^\beta$, $Y_R = I_R\Omega_{eq}/m_e c^2\varepsilon^\beta$,

$$\tau = \Omega_{eq}\varepsilon^\beta\int^t w(t')dt',$$

(i.e., $(w(t)\Omega_{eq}\varepsilon^\beta)d/d\tau = d/dt$ and integration is along electron trajectories) and rewrite Eqs. (7) as

$$\frac{dY}{d\tau} = -\varepsilon^{1-3\beta/2}\sqrt{2Y}u\cos\varphi \quad (8)$$
$$\frac{d\varphi}{d\tau} = (Y-Y_R) + \frac{\varepsilon^{1-3\beta/2}}{\sqrt{2Y}}u\sin\varphi$$

Equations (8) are Hamiltonian equations for

$$H_Y = \frac{1}{2}\left(Y-Y_R\right)^2 + \varepsilon^{1-3\beta/2}\sqrt{2Y}u\sin\varphi \quad (9)$$

If $\varepsilon^{1-3\beta/2} \ll 1$ (i.e., $\beta > 2/3$), then the Hamiltonian system resembles the general system with small perturbations $\sim \sin\varphi$ and the standard approach is applicable for description of such system[12,55]. Thus, we are interested in system with $\beta = 2/3$ and Hamiltonian

$$H_Y = \frac{1}{2}\left(Y-Y_R\right)^2 + \sqrt{2Y}u\sin\varphi \quad (10)$$

Hamiltonian (10) does not contain small parameters, but coefficients u, Y_R depend on slow variables. To describe dynamics of Hamiltonian system (10), we introduce new variables $p = \sqrt{2Y}\cos\varphi$, $q = \sqrt{2Y}\sin\varphi$ with

$$\frac{\partial q}{\partial\varphi}\frac{\partial p}{\partial Y} - \frac{\partial q}{\partial Y}\frac{\partial p}{\partial\varphi} = 1$$

Thus, (q, p) are new canonical coordinate and momentum, and new Hamiltonian takes the form

$$F = \frac{1}{2}\left(\frac{1}{2}p^2 + \frac{1}{2}q^2 - Y_R\right)^2 + uq \quad (11)$$

The principal dynamics of Hamiltonian system (11) has been described in Ref. 50 (see also Ref. 30).

Let us consider a profile of Hamiltonian (11) on the axis $p = 0$: $U = F_{p=0} = (1/2)(q^2/2 - Y_R)^2 + uq$. Equation determining extrema of $U(q)$ function is $dU/dq = (1/2)q^3 - Y_R q + u = 0$, that can be rewritten as $(1/2)\tilde{q}^3 - (2/3)\tilde{q}(Y_R/Y_R^*) + 1 = 0$ with $\tilde{q} = q/u^{1/3}$ and $Y_R^* = (3/2)u^{2/3}$. Figure 2(a) shows that for $Y_R < Y_R^*$ there is only one extremum and for $Y_R > Y_R^*$ there are two extrema of $U(q)$. Therefore, the phase portrait of Hamiltonian (11) have two types shown in Fig 2(b): for $Y_R < Y_R^*$ there is only one O-point in the phase plane and phase trajectories rotate around this point, whereas for $Y_R > Y_R^*$ there are two O-points and X-point (saddle point), and two separatrices $\ell_{1,2}$ demarcate the phase portrait onto three domains G_{outer}, G_{inner}, G_{inter} (see also Ref. 30 and 50).

For constant u, Y_R system (11) is integrable one, whereas for slowly changing u, Y_R we can introduce an adiabatic invariant $I_p = (2\pi)^{-1}\oint pdq$ (because all phase trajectories in the portrait shown in Fig. 2(b) are closed; see Ref. 43). In absence of separatrix (for $Y_R < Y_R^*$), I_p would conserve with the exponential accuracy $\sim \exp\left(-\varepsilon^{-1/3}\right)$ where $\varepsilon^{1/3} \ll 1$ separates time-scales of u, Y_R change (s, P change) and p, q change[43,51]. For conserved I_p the system becomes integrable and Y well before the resonance equals to Y well after the resonance. Note $I_p = (2\pi)^{-1}\oint pdq = 2Y(2\pi)^{-1}\oint\cos^2\varphi d\varphi = Y$ far from $\ell_{1,2}$ or in absence of $\ell_{1,2}$.

For phase trajectories crossing the separatrices in the phase portrait from Fig. 2(b), there is a change of I_p (see Refs. 16, 52, and 54). This change can be separated into so-called *dynamical* jump $\sim \varepsilon^{1/3}\ln\varepsilon^{1/3}$ and *geometrical* jump $\sim O(1)$ (see details in reviews 9 and 53). The geometrical jump is much larger than dynamical one.

The separatrix crossing results in particle transition from the region with area $2\pi I_{p,init}$ ($I_{p,init}$ is the initial value of I_p) to the region with another area S. At the moment of the separatrix crossing the invariant I_p becomes equal to $S/2\pi$. Thus, there is a jump $\Delta I_p = \Delta S/2\pi = S/2\pi - I_{p,init}$. This jump directly relates to the jump of I_x of the initial system (1)

$$\Delta I_x = \Delta I = \frac{m_e c^2\Delta Y}{\Omega_{eq}\varepsilon^{-2/3}} = \frac{m_e c^2\Delta S}{2\pi\Omega_{eq}}\left(\frac{eB_w}{m_e c^2 k_{eq}}\right)^{2/3} \quad (12)$$

Therefore, to describe electron scattering in system (1) with small I_x (small I), we should describe I_p change due to separatrix crossing on the phase portrait shown in Fig. 2(b).

IV. DYNAMICS OF SYSTEM (11)

Let us study properties of Hamiltonian (11) that are important for evaluation of the ΔI_p jump. First, we are interested in areas of regions G_{inner}, G_{inter}, G_{outer}. Coordinates of X-point C in the (q,p) plane are $(q_c,0)$ where q_c is the maximum root of equation $dU/dq = (1/2)q^3 - Y_R q + u = 0$. We introduce polar coordinates (ρ,η) as $q = q_c + \rho\cos\eta$, $p = \rho\sin\eta$ and rewrite Hamiltonian (11) as

$$F = \frac{1}{2}\left(\frac{1}{2}\rho^2 + \frac{1}{2}q_c^2 - Y_R\right)^2 + \frac{1}{2}q_c^2\rho^2\cos^2\eta + \frac{1}{2}\rho^3 q_c\cos\eta + uq_c \tag{13}$$

Then, separatrices $\ell_{1,2}$ are defined by equation $F = F_{\rho=0}$:

$$\rho^2 + 4\rho q_c\cos\eta + 4q_c^2\cos^2\eta + 4\left(\frac{q_c^2}{2} - Y_R\right) = 0 \tag{14}$$

with the solution

$$\rho_\pm = -2q_c\cos\eta \pm 2\sqrt{Y_R - \frac{1}{2}q_c^2} \tag{15}$$

Areas of G_{inner}, G_{inter}, and G_{outer} are given by equations:

$$S_{inner} = \frac{1}{2}\oint \rho_-^2 d\eta = \int_{\eta_-}^{\pi}\rho_-^2 d\eta = 4Y_R\eta_c - 3q_c^2\sin 2\eta_c$$

$$S_{outer} = \frac{1}{2}\oint \rho_+^2 d\eta = \int_{\eta_+}^{\pi}\rho_+^2 d\eta = 4Y_R(\pi-\eta_c) + 3q_c^2\sin 2\eta_c$$

$$S_{inter} = \frac{1}{2}\oint \left(\rho_+^2 - \rho_-^2\right)d\eta = S_{outer} - S_{inner}$$
$$= 4Y_R(\pi - 2\eta_c) + 6q_c^2\sin 2\eta_c \tag{16}$$

where

$$\int_{\eta_\pm}^{\pi}\rho_\pm^2 d\tilde\eta = 4q_c^2\int_{\eta_\pm}^{\pi}\cos^2\eta d\tilde\eta - 4\left(\frac{1}{2}q_c^2 - Y_R\right)(\pi-\eta_\pm)$$

$$\mp 8q_c\sqrt{Y_R - \frac{1}{2}q_c^2}\int_{\eta_\pm}^{\pi}\cos\tilde\eta d\tilde\eta = 4Y_R(\pi-\eta_\pm) - q_c^2\sin 2\eta_\pm$$

$$\pm 8q_c\sqrt{Y_R - \frac{1}{2}q_c^2}\sin\eta_\pm = 4Y_R(\pi-\eta_\pm) + 3q_c^2\sin 2\eta_\pm$$

$$= \begin{cases} 4Y_R(\pi-\eta_c) + 3q_c^2\sin 2\eta_c & \eta_+ = \eta_c \\ 4Y_R\eta_c - 3q_c^2\sin 2\eta_c & \eta_- = \pi - \eta_c \end{cases}$$

and $q_c\cos\eta_c = \sqrt{Y_R - q_c^2/2}$ (solution of $\rho_+ = 0$, i.e. we take $\eta_c < \pi/2$, see Fig. 3(a)).

Introducing $\tilde q_c = q_c/u^{1/3}$ and $y_R = Y_R/Y_R^*$ (where $Y_R^* = (3/2)u^{2/3}$), we rewrite Eqs. (16) as

$$S_{inner} = \tilde S_{inner}4Y_R^*,\quad \tilde S_{inner} = y_R\eta_c - \tilde q_c^2\sin\eta_c\cos\eta_c$$
$$S_{outer} = \tilde S_{outer}4Y_R^*,\quad \tilde S_{outer} = y_R(\pi-\eta_c) + \tilde q_c^2\sin\eta_c\cos\eta_c$$
$$S_{inter} = \tilde S_{inter}4Y_R^*,\quad \tilde S_{inter} = y_R(\pi-2\eta_c) + \tilde q_c^2\sin 2\eta_c$$
$$\eta_c = \arccos\sqrt{\frac{3}{2}\frac{y_R}{\tilde q_c^2} - \frac{1}{2}} = \arccos\left(\tilde q_c^{-3/2}\right) \tag{17}$$

and $\tilde q_c^3 - 3\tilde q_c y_R + 2 = 0$. Figures 3(b,c) shows $\tilde q_c$, $\cos(\eta_c)$, and areas $\tilde S_{inner}$, $\tilde S_{outer}$, $\tilde S_{inter}$ as function of y_R parameter.

V. ELECTRON SCATTERING

Figure 3(c) shows that areas S_{inner}, S_{outer}, S_{inter} evolve with $y_R = Y_R/Y_R^*$, but y_R is the function of slow time (slow variables) and evolves along the electron trajectory:

$$y_R = \frac{Y_R}{Y_R^*} = \frac{2}{3}\frac{I_R\Omega_{eq}}{m_ec^2(u\varepsilon)^{2/3}} = \frac{2}{3}\frac{\kappa^{2/3}k^2c^2}{\gamma_0^{4/3}\Omega_{ce}^2}\frac{I_R\Omega_{ce}}{m_ec^2(B_w/B)^{2/3}} \tag{18}$$

where

$$\frac{K^2c^2}{\Omega_{ce}^2} = \frac{\kappa}{\gamma_0^3}\frac{k^2c^2}{\Omega_{ce}^2} \tag{19}$$
$$\kappa = 1 - \frac{\Omega_{ce}^2}{k^2c^2} - 2\frac{\Omega_{ce}}{kc}\frac{P}{m_ec} = \gamma_0^2 - \left(\frac{\Omega_{ce}}{kc} + \sqrt{\gamma_0^2-1}\right)^2$$
$$(u\varepsilon)^{2/3} = \frac{\gamma_0^{4/3}}{\kappa^{2/3}}\left(\frac{\Omega_{ce}^2}{k^2c^2}\frac{eB_w}{m_ec^2k}\right)^{2/3}\frac{\Omega_{eq}}{\Omega_{ce}}$$

The resonant interaction starts with $I_R = I_x$ (initial I value is I_x), and for this moment we can write

$$y_R = \frac{2}{3}\frac{\kappa^{2/3}k^2c^2}{\gamma_0^{4/3}\Omega_{ce}^2}\frac{I_x\Omega_{ce}}{m_ec^2(B_w/B)^{2/3}} \tag{20}$$
$$\kappa = \gamma_0^2\left(1 - (\omega/kc)^2\right) \tag{21}$$

The factor $\sim 2I_x\Omega_{ce}/m_ec^2(B_w/B)^{2/3}$ is of the order of one due to smallness of I_x. In the resonance y_R variation is described by Eq. (18) with I_R given by Eq. (6).

Figure 4(a) shows y_R variation with the magnetic latitude for particles moving from high latitudes toward the equatorial plane. Along the resonant trajectories y_R increases, i.e. normalized areas $\tilde S_{inner}$, $\tilde S_{outer}$, and $\tilde S_{inter}$ should grow (see Fig. 3(c)). However, expression of

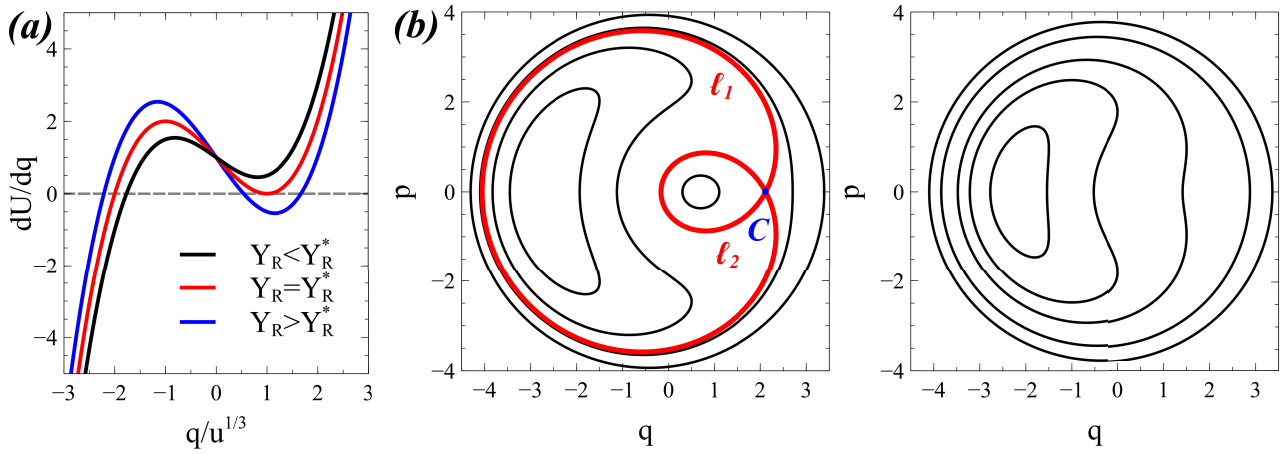

FIG. 2: (a) Profiles of $dU/dq = \tilde{q}^3/2 - (3/2)\tilde{q}(Y_R/Y_R^*) + 1$ for different Y_R; $Y_R^* = (3/2)u^{2/3}$ and $\tilde{q} = q/u^{1/3}$. (b) Phase portraits of system (11) with $u = 2$ for $Y_R > Y_R^*$ (left) and $Y_R < Y_R^*$ (right). Bold red curve shows the separatrices $\ell_{1,2}$.

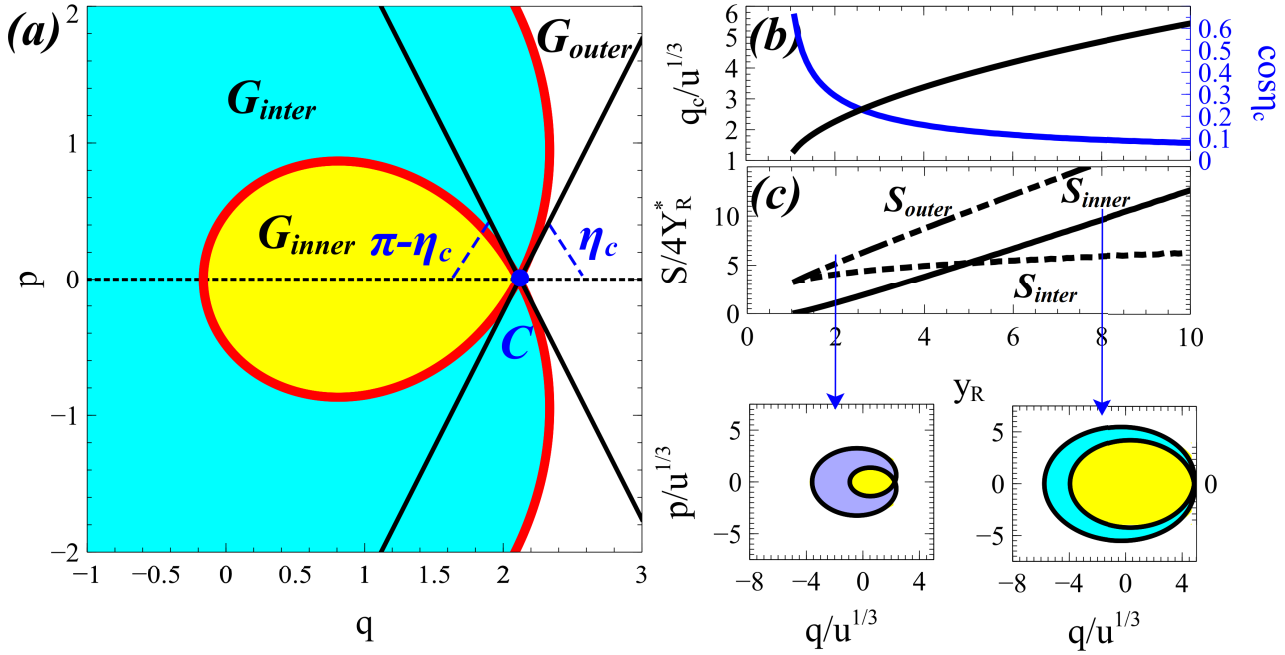

FIG. 3: (a) Schematic of G_{inner}, G_{inter}, and G_{outer} regions; angle η_c is shown. (b) and (c) Profiles of $\tilde{q}_c$, $\cos\eta_c$, $\tilde{S}_{inner} = S_{inner}/4Y_R^*$, $\tilde{S}_{outer} = S_{outer}/4Y_R^*$, and $\tilde{S}_{inter} = S_{inter}/4Y_R^*$; bottom panels show phase portraits for two $y_R = Y_R/Y_R^*$ values.

$S = 4Y_R^*\tilde{S}$ includes the wave amplitude u ($Y_R^* \sim u^{2/3}$) that generally drops to zero at the equatorial plane. Thus, S dynamics along the resonant trajectories is determined by the competition of $\tilde{S}$ increase and Y_R^* decrease. Figure 4(b) shows that S_{inter} decreases, whereas S_{inner} increases. Taking into account that y_R grows from values is smaller than one (i.e. from values for which $S_{inner} = 0$ and there is only S_{outer}; see Fig. 3(c)), we describe resonant particle dynamics.

Far from the resonance, Y equals to $\Omega_{eq}I_x/m_ec^2\varepsilon^{2/3}$ and equals to $I_p = (2\pi)^{-1}\oint pdq$ for Hamiltonian system (11). Thus, for given I_x, in the (p, q) plane electrons are distributed along the circle with the radius $\sqrt{2Y}$; the entire circle is inside the region G_{outer}, because G_{inner} and G_{inter} do not exist (see schematic in Fig. 4(c), moment #1). With time (or with y_R increase) regions G_{inner}, G_{inter} form (when y_R exceeds one), whereas trajectories on the (q, p) plane deform, but save their areas. Then two scenarios are possible.

A. Scenario for small Y

If initial Y is sufficiently small, at the moment of $G_{inner,inter}$ formation trajectories appear inside G_{inter} (Fig. 4(c), moment #2 shows such red trajectory within G_{inte}). From this moment and up to the sepatrix crossing the particle is in the resonance with the wave. When decreasing $S_{inter}/2\pi$ reaches I_p, electrons cross the separatrix ℓ_2 and appear in G_{inner} region (S_{outer} increases with S_{inter}, and electrons cannot come to G_{outer}) with growing S_{inner} (see schematic in Fig. 4(c), moment #3). This separatrix crossing results in a jump of the adiabatic invariant $\Delta I_p = (S_{inner} - S_{inter})/2\pi$ where S_{inner} is evaluated at the moment when $S_{inter} = 2\pi I_p$ (escape from the resonance). A new I_p would be conserved, and far from the separatrix crossing (far from the resonance) new Y is equal to new I_p. Thus, the jump of Y equals to $\Delta Y = (S_{inner} - S_{inter})/2\pi = 4Y_R^*(\tilde{S}_{inner} - \tilde{S}_{inter})/2\pi$ where Y_R^* is evaluated at the moment of the separatrix crossing (that can be quite far from the resonance when G_{inter} forms). Jump ΔY can be rewritten as a jump of I_x, see Eq. (13):

$$\Delta I_x = \frac{\Delta\tilde{S}}{2\pi}\frac{4Y_R^* m_e c^2 \varepsilon^{2/3}}{\Omega_{eq}} = \frac{3\Delta\tilde{S}}{\pi}\frac{m_e c^2}{\Omega_{eq}}\left(u\varepsilon\right)^{2/3}$$
$$= \frac{3\Delta\tilde{S}}{\pi}\frac{m_e c^2}{\Omega_{ce}}\frac{\gamma_0^{4/3}\Omega_{ce}^2}{\kappa^{2/3}k^2c^2}\left(B_w/B\right)^{2/3} \qquad (22)$$

where all variables changing along magnetic field line should be evaluated at the separatrix crossing moment.

B. Scenario for large Y

If initial Y is sufficiently large, then at the moment of $G_{inner,inter}$ formation the electron trajectories in the (q,p) plane appear in G_{outer}. For such trajectories the separatrix crossing would results in $\Delta Y = (S_{inner} - S_{outer})/2\pi$. Because $S_{outer} > S_{inner}$, this Y change (and I_x change) would mean I_x decrease, i.e. this is classical nonlinear electron scattering on the resonance[7,12,66].

C. Electron drift in pitch-angle space

Let us summarize results of I_p (Y) changes. The separatrix crossing by trajectory in the (q,p) plane occurs when $S_{inter} = 2\pi I_p$, and thus the moment of crossing depends on I_p (i.e. on the initial Y or, equivalently, on initial I_x). There are two possible situations shown in Fig. 5.

If the initial I_x (initial $I_p = S_{inter}/2\pi$) is sufficiently small, then the separatrix crossing occurs when electron orbits are in G_{inter} and $S_{inter} < S_{inner}$ (this moment is is quite far from the moment of G_{inter} forming, i.e.. particles spend a significant time $\sim O(\varepsilon^{1/3})$ in the resonance before the separatrix crossing). Thus, jump $\Delta I_p = (S_{inner} - S_{inter})/2\pi > 0$ and I_x increases due to the electron resonant interaction with the waves (see Fig. 5(a) and black trajectories in Fig. 1, right panels). Magnitude of I_x change is defined by Eq. (22).

If the initial I_x (initial I_p) is sufficiently large, then the separatrix crossing occurs when electron orbits are in G_{outer}. This happens right around the resonance, i.e. particles do not spend a long time being trapped in G_{outer}. Thus, jump $\Delta I_p = (S_{inner} - S_{outer})/2\pi < 0$ (because $S_{outer} > S_{inner}$) and I_x decreases due to the electron resonant interaction with the waves (see Fig. 5(b) and black trajectories in Fig. 1, left panels).

These two situations explain classical scattering with I_x decrease for electrons having not-too-small I_x (see Refs. 7 and 66) and anomalous scattering with I_x increase for electrons with initial very small I_x (see Refs. 25, 40, and 47).

VI. DISCUSSION

Whistler-mode waves nonlinearly scatter field-aligned (small-I_x) electrons away from the loss-cone[47], and this effect is responsible for *electron trapping around loss-cone*[40]. Such nonlinear scattering of field-aligned electrons differs significantly from nonlinear scattering of moderate pitch-angle electrons toward the loss-cone.

Similar effect of the change of electron scattering direction has been found for electromagnetic ion cyclotron waves. These waves nonlinearly scatter moderate pitch-angle electrons away from the loss-cone[6,27,28], but for field-aligned (small-I_x) electrons this nonlinear scattering results in electron pitch-angle decrease (the effect is called *direct scattering*, see detailed analysis in Ref. 29, and references therein). As we show in this study, such modification of nonlinear scattering for small I_x can be described analytically, because even for small I_x there is separation of time-scales of (φ, I) variations and $(s, p_\parallel)$ variations. Let us discuss obtained results, and summarize them in the Conclusion.

A. Electron dynamics around loss-cone

Figure 5 shows that for some initial $I_x = I_x^*$, the separatrix crossing occurs with $\Delta I_x = 0$, i.e. $S_{inter} \approx S_{inner}$. Thus, electrons with this I_x^* would not be nonlinear scattered (in the leading approximation). Let us consider a realistic system with $I_x^* \sim \varepsilon^{2/3}$ sufficiently small to keep derived equations valid. Change of I_x can be written as $\Delta I_x = \Delta\alpha_{eq}\sin\alpha_{eq}\cos\alpha_{eq} m_e c^2(\gamma^2 - 1)/(\Omega_{eq} - \sin^2\alpha_{eq}\omega\gamma)$ where α_{eq} is the electron equatorial pitch-angle. We denote α_{eq}^* value of pitch-angle for which $I_x = I_x^*$ (for given energy γ), and write $\Delta\alpha_{eq} = 2\Delta I_x \Omega_{eq}/m_e c^2 \sin 2\alpha_{eq} \approx (\alpha_{eq} - \alpha_{eq}^*)\nu'$ where $\nu' = \partial\nu/\partial\alpha_{eq}|_{\alpha_{eq}=\alpha_{eq}^*}$ and $\nu = 2\Delta I_x(\alpha_{eq})\Omega_{eq}/m_e c^2 \sin 2\alpha_{eq}$ with $\nu(\alpha_{eq}^*) = 0$.

Figure 6 shows two possible variants of field-aligned (small I_x) electron scattering. Independently on ν', elec-

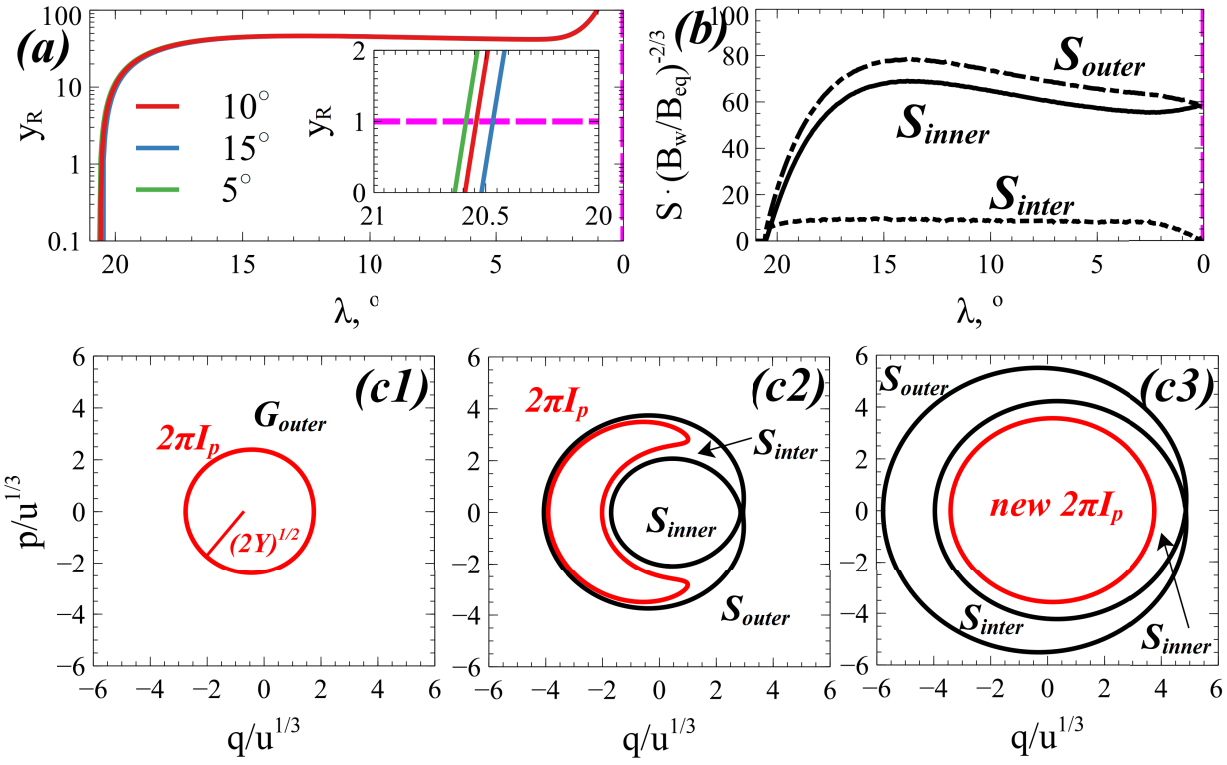

FIG. 4: (a) y_R as a function of magnetic latitude for 50 keV energy and three pitch-angles. (b) Areas $S_{inner,inter,outer}$ as functions of magnetic latitude for 50 keV, 10° pitch-angle. Details of wave model are the same as in the caption of Fig.1. (c) three schematic views of particle trajectories in the (q,p) plane. Phase portraits change from c1 to c3 along particle trajectory.

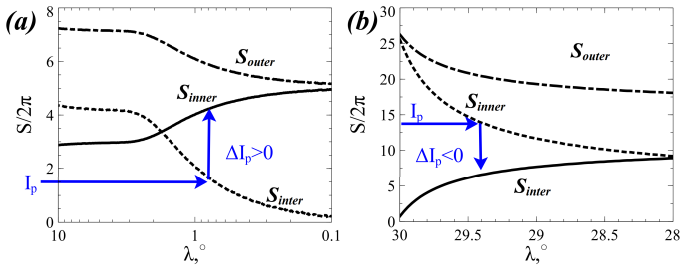

FIG. 5: Schematic of I_p jumps due to separatrix crossing. (a) System with positive ΔI_p; (b) System with negative ΔI_p. For simplicity we use $I_R \approx I_x$ here.

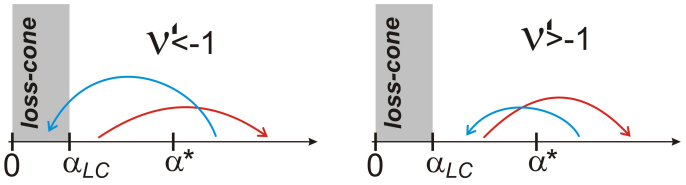

FIG. 6: Schematic view of pitch-angle jumps for system with electron losses (left panel, $\nu' < -1$) and system without electron losses (right panel, $\nu' > -1$).

trons with $\alpha_{eq} < \alpha^*_{eq}$ are nonlinearly scattered with pitch-angle increase, i.e. scattered away from the loss-cone α_{LC}. Therefore, the nonlinear scattering into loss-cone (electron precipitations) would require that electron with $\alpha_{eq} > \alpha^*_{eq}$ are scattered with sufficiently large $\Delta\alpha_{eq}$: $\alpha_{eq} + \Delta\alpha_{eq} < \alpha_{LC}$. If $\nu' < -1$, $\alpha_{eq} + \Delta\alpha_{eq} < \alpha_{LC}$ can be rewritten as $\alpha_{eq} \geq (|\nu'|\alpha^*_{eq} - \alpha_{LC})/(|\nu'| - 1)$, and this inequality is always satisfied for $\alpha_{eq} > \alpha^*_{eq}$ and sufficiently small loss-cone $\alpha_{LC} < 1$. Thus, for $\nu' < -1$ there are electron nonlinear scattering into loss-cone and precipitations. If $\nu' > -1$, $\alpha_{eq} + \Delta\alpha_{eq} < \alpha_{LC}$ can be rewritten as $\alpha_{eq} \leq (\alpha_{LC} - |\nu'|\alpha^*_{eq})/(1 - |\nu'|)$, and this inequality is satisfied for $\alpha_{eq} > \alpha^*_{eq}$ only for the exotic case $\alpha_{LC} > \alpha^*_{eq}$. Thus, if $\nu' > -1$ there are no electron scattering into loss-cone and no precipitations (such regime is called *electron trapping around loss-cone*, see Ref. 40). These estimates demonstrate that the nonlinear scattering of small pitch-angle electrons with $\Delta I_x > 0$ does not necessary stop electron precipitations.

The pitch-angle jump $\Delta\alpha_{eq}$ is proportional to ΔI_x given by Eq. (22), and thus there is a scaling $\Delta\alpha_{eq} \sim B_w^{2/3}$. If α^*_{eq} depends on B_w sufficiently weakly, then the wave amplitude increase would result in $|\nu'|$ increase. Therefore, for sufficiently high B_w we should expect the regime with electron nonlinear scattering into loss-cone (see Fig. 6, left panels). To check this scenario, we integrate numerically set of electron trajectories given by

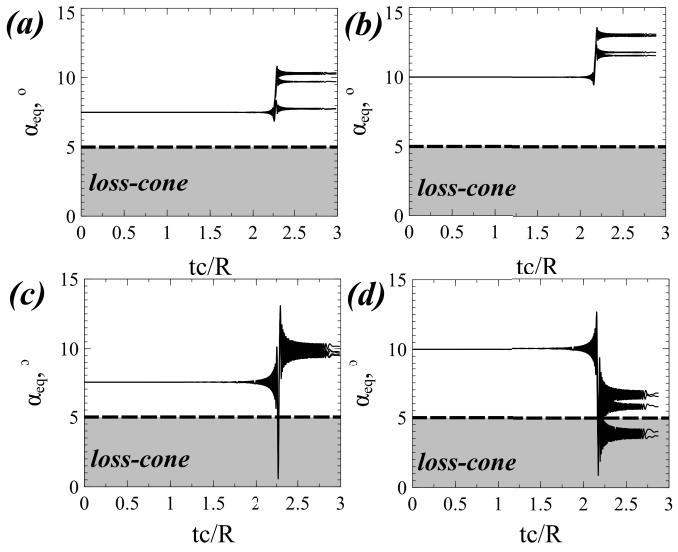

FIG. 7: Pitch-angle change along electron trajectories for $L = 4$ (see details of the wave model in the caption of Fig. 1). Panels (a) and (b) shows trajectories for $B_w = 250$ pT; panels (c) and (d) shows trajectories for $B_w = 1500$ pT (note only scattered electron trajectories are shown, and trapped electron trajectories are excluded). The loss-cone is shown for illustration, $\alpha_{LC} \approx 5°$.

Hamiltonian equations (2) for the same initial γ and two wave amplitudes. Figure 7 shows that for large B_w electrons can be scattered into loss-cone and precipitate.

B. Two types of phase portraits

We consider resonant nonlinear scattering of electrons with small I_x, for which the resonant Hamiltonian takes the form given by Eq. (10) or Eq. (11). Let us compare this Hamiltonian with one describing the classical problem of charged particle scattering for moderate I_x values (see Refs. 7 and 66). Instead of expansion of Hamiltonian (3) around $I = 0$, we can expand it around the resonant value $I = I_{res}(s, P)$ determined from $\partial H/\partial I = 0$ equation:

$$H = -\omega I_{res} + \gamma_{res} + \frac{1}{2m_e} K_{res}^2 \left(I - I_{res}\right)^2 + \sqrt{\frac{2I_{res}\Omega_{ce}}{m_e}} \frac{eB_w}{ck\gamma_{res}} \sin\varphi \qquad (23)$$

where $K_{res} = \partial^2 H/\partial I^2|_{I=I_{res}}$ and $\gamma_{res} = \gamma|_{I=I_{res}}$. The main difference of this Hamiltonian and one from Eq. (4) is that the effective wave amplitude does not depend on I in Eq. (23). The phase portrait of Hamiltonian (23) with frozen slow variables is shown in Fig. 8(a).

Instead of introducing (q, p) coordinates it is more convenient to introduce $P_\phi = I - I_{res}$ through the generation function $W = (I - I_{res})\varphi + Ps^*$ with new slow variables $s^* = s + (\partial I_{res}/\partial P)\varphi$, $P^* = P - (\partial I_{res}/\partial P)\varphi$. Expanding $I_{res}(s, P)$ and $\gamma_{res}(s, P)$ over $(\partial I_{res}/\partial P)$, $(\partial I_{res}/\partial s)$, we rewrite Hamiltonian (23) as

$$H \approx -\omega I_{res} + \gamma_{res} + \frac{K_{res}^2 P_\varphi^2}{2m_e} - \{\gamma_{res}, I_{res}\}\,\varphi + \sqrt{\frac{2I_{res}\Omega_{ce}}{m_e}} \frac{eB_w}{ck\gamma_{res}} \sin\varphi \qquad (24)$$

where $\{\dots\}$ are Poisson brackets, and all function in Eq. (24) depend on (s^*, P^*). The phase portrait of Hamiltonian (24) with the frozen slow variables (s^*, P^*) is shown in Fig. 8(b). This is the classical portrait of the pendulum with torque[9] with three main phase space regions: before resonance $P_\varphi = 0$ crossing particles are in G_{outer}, and resonance crossing can result in trapping (particles appear in G_{inter}) or scattering (particles appear in G_{inner}). Therefore, there is direct relation between three regions $G_{outer,inner,inter}$ of Hamiltonian of (11) and Hamiltonian (24).

For the initial system given by Eq. (3) nonlinear scattering (transition from G_{outer} to G_{inner}) always appears with I_x decrease, and this effect is well seen in the phase portrait (c) of Fig. 8: the area S_{outer} is always larger than the area S_{inner}. But when the initial invariant I_x (I_p or $I_\varphi = (2\pi)^{-1} \oint P_\varphi d\varphi$) is sufficiently small, particles become trapped within region G_{inter} as soon as this region appears during particle motion along their trajectories. In phase portrait (c) of Fig. 8 this trapping means that the area surrounded by the particle trajectory $2\pi I_p \approx 2\pi Y$ is smaller than S_{inter} at the moment when G_{inter} appears (when y_R becomes larger than one, see Fig. 3(c)). For $y_R = 1$ we get $\eta_c = 0$, $\tilde{q}_c = 1$, and $S_{inter} = 4\pi Y_R^*$. Thus, the threshold I_x value is $2I_x\Omega_{ce}/m_e c^2 = 3(\Omega_{ce}/kc)^2(B_w/\kappa B)^{2/3}$.

This is so-called *autoresonance* phenomena of the 100% trapping in the resonant systems (see, e.g., Refs. 21, 22, and 57 and references therein). Being trapped into G_{inter}, particles can both increase or decrease their I_p (and I_x) during the transition from G_{inter} to G_{inner}: the I_x change depends on the ratio of S_{inter}/S_{inner} at the moment when S_{inter} becomes equal to $2\pi I_p$. For sufficiently small I_p (small I_x), the ratio $S_{inter}/S_{inner} = 2\pi I_p/S_{inter}$ will be below one, and particles will increase their I_p (and I_x) due to the resonant interaction. Formally, this interaction cannot be called scattering, because particles are trapped into G_{inter} from the beginning.

C. Small I_x for electrons resonating with electrostatic waves

For resonances in inhomogeneous plasma, there is the direct analogy between electron interaction with whistler-mode waves and with electrostatic waves[26,36,37,44,58]. Therefore, we can expect a change of the regime of nonlinear electron scattering (phase bunching) by electrostatic waves for field-aligned electrons.

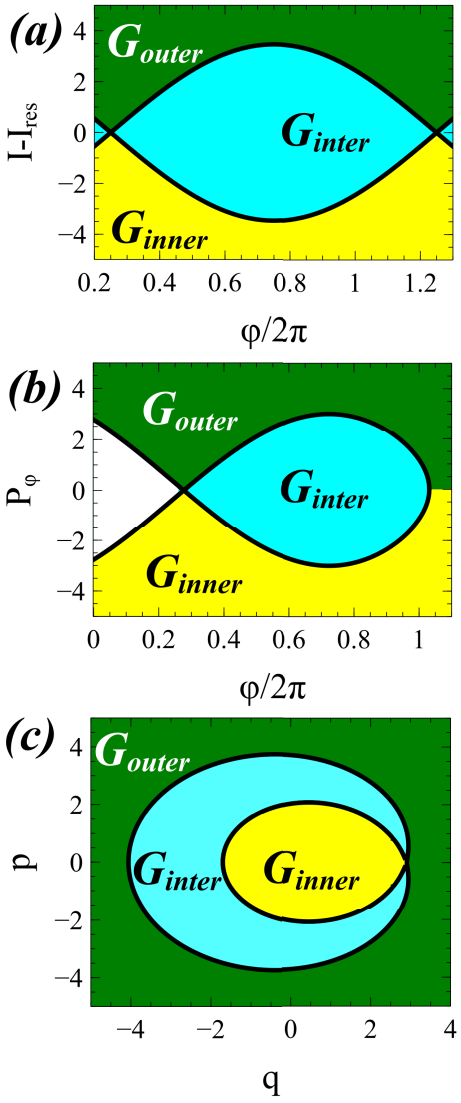

FIG. 8: Phase portraits of Hamiltonian (23), panel (a), of Hamiltonian (24), panel (b), and Hamiltonian (11), panel (c).

The main difference between the cyclotron resonance with electromagnetic waves (e.g., whistler-mode waves) and the Landau resonance with electrostatic waves is that for electrostatic waves the wave amplitude $U_w = e\Phi_w$ is determined by the electric field potential Φ_w and does not depend on I_x. Thus, Eqs. (7) would take the form:

$$\dot{I} = -e\Phi_w \cos\varphi, \quad \dot{\varphi} = \frac{1}{m_e} K^2 (I - I_R) \tag{25}$$

Defining a small parameter $\varepsilon = e\Phi_w/m_e c^2$ (the analog of $eB_w/m_e c^2 k_{eq}$ used through the paper), we can estimate the threshold value of I_x for which there is no time separation of I and φ variations in Eqs. (25). For $\tau \sim t\varepsilon^\beta$ and $Y \sim I\varepsilon^{-\beta}$, Eqs. (25) give $\beta = 1/2$. Thus, instead of the scaling $I_x \sim (eB_w/k)^{2/3}$ for the cyclotron resonance, we obtain the scaling $I_x \sim (e\Phi_w)^{1/2}$ for the Landau resonance.

Electrons can resonate with whistler mode waves through the Landau resonance, if waves are obliquely propagating, i.e. if there is a finite angle θ between a wavevector and a background magnetic field. For a general case of $\theta \neq 0$, the whistler-mode wave amplitude in Hamiltonian (3) takes the form[2,13,61,70]:

$$U_w = \sqrt{\frac{2I_x\Omega_{ce}}{m_e c^2}} \frac{eB_w}{k} \sum_{\pm} \frac{\cos\theta \pm C_1}{2\gamma} J_{n\pm1}\left(\sqrt{\frac{2I_x k^2}{m_e\Omega_{ce}}}\sin\theta\right) \tag{26}$$
$$+ \frac{eB_w}{k}\left(\frac{p_\parallel}{\gamma m_e c} + C_2\right) J_n\left(\sqrt{\frac{2I_x k^2}{m_e\Omega_{ce}}}\sin\theta\right)\sin\theta$$

where n is the resonance number, $C_{1,2}$ are functions of wave dispersion and θ, and J_n are Bessel functions. Equation (26) shows that for the cyclotron resonance $n = -1$ and small I_x we have $U_w \sim \sqrt{I_x}$, and thus $I_x \sim (eB_w/k)^{2/3}$ scaling works. For the Landau resonance $n = 0$ and small I_x we have $U_w \sim \sin\theta \cdot (const + I_x) \sim O(I_x)$, and thus $I_x \sim (eB_w/k)^{1/2}$ scaling works.

VII. CONCLUSIONS

In this study we propose the theoretical model of nonlinear resonant scattering (phase bunching) of small pitch-angle electrons in the inhomogeneous magnetic field. Basic parameters and wave characteristics correspond to whistler-mode waves in the Earth's radiation belts. Using the adiabatic invariant I_x (magnetic moment $\mu = eI_x/c$) and the small system parameter $\varepsilon \approx eB_w/m_e c^2 k$), we show that

- The threshold value of I_x for a new regime of electron nonlinear scattering away from the loss-cone is scaling with ε as: $I_x\Omega_{ce}/m_e c^2 \sim \varepsilon^{2/3}$. For I_x smaller than this threshold value, the model of electron resonant interaction should include $\sim \sqrt{I_x}$ factor for the wave amplitude.

- For I_x below the threshold value, the I_x change due to nonlinear resonant scattering is $\Delta I_x\Omega_{ce}/m_e c^2 \sim (kc/\Omega_{ce})^{2/3}\varepsilon^{2/3}$, whereas the precise system dynamics is described by theory of separatrix crossing given by Refs. 30 and 50.

We also should note that the proposed theoretical model describes the ideal system with the monochromatic coherent whistler-mode wave. A wave field modulation is known to influence significantly the nonlinear resonant interaction[11,25,29,31,49,60,72]. Thus, to understand relevance of the proposed model to the electron scattering in the Earth's radiation belts, a more systematic numerical investigation of electron scattering for realistic short wave-packets whistler-mode waves[79,80] is needed.

ACKNOWLEDGMENTS

A.V.A. are thankful to M. Kitahara and Y. Katoh for pointing on the problem of the nonlinear scattering of small pitch-angle electrons[40], to V. Grach and A. Demekhov for very useful discussion of their results on EMIC waves scattering[27–29], to D. Shklyar for discussion of initial research of this problem[47], and to D. Mourenas for useful suggestions. Work of A.V.A. and A.I.N. was supported by the Russian Scientific Foundation, project 19-12-00313. A.I.N. also was supported by the Leverhulme Trust, project RPG-2018-143. **TODO:** Wen, please, add more references/info here

[1] Agapitov, O.V., Artemyev, A., Krasnoselskikh, V., Khotyaintsev, Y.V., Mourenas, D., Breuillard, H., Balikhin, M., Rolland, G., 2013. Statistics of whistler mode waves in the outer radiation belt: Cluster STAFF-SA measurements. J. Geophys. Res. 118, 3407–3420. doi:doi:10.1002/jgra.50312.

[2] Albert, J.M., 1993. Cyclotron resonance in an inhomogeneous magnetic field. Physics of Fluids B 5, 2744–2750. doi:doi:10.1063/1.860715.

[3] Albert, J.M., 2000. Gyroresonant interactions of radiation belt particles with a monochromatic electromagnetic wave. J. Geophys. Res. 105, 21191. doi:doi:10.1029/2000JA000008.

[4] Albert, J.M., 2001. Comparison of pitch angle diffusion by turbulent and monochromatic whistler waves. J. Geophys. Res. 106, 8477–8482. doi:doi:10.1029/2000JA000304.

[5] Albert, J.M., 2010. Diffusion by one wave and by many waves. J. Geophys. Res. 115, 0. doi:doi:10.1029/2009JA014732.

[6] Albert, J.M., Bortnik, J., 2009. Nonlinear interaction of radiation belt electrons with electromagnetic ion cyclotron waves. Geophys. Res. Lett. 36, 12110. doi:doi:10.1029/2009GL038904.

[7] Albert, J.M., Tao, X., Bortnik, J., 2013. Aspects of Nonlinear Wave-Particle Interactions, in: Summers, D., Mann, I.U., Baker, D.N., Schulz, M. (Eds.), Dynamics of the Earth's Radiation Belts and Inner Magnetosphere. doi:doi:10.1029/2012GM001324.

[8] Andronov, A.A., Trakhtengerts, V.Y., 1964. Kinetic instability of the Earth's outer radiation belt. Geomagnetism and Aeronomy 4, 233–242.

[9] Arnold, V.I., Kozlov, V.V., Neishtadt, A.I., 2006. Mathematical Aspects of Classical and Celestial Mechanics. Dynamical Systems III. Encyclopedia of Mathematical Sciences. 3rd ed., Springer-Verlag, New York.

[10] Artemyev, A.V., Agapitov, O., Mourenas, D., Krasnoselskikh, V., Shastun, V., Mozer, F., 2016. Oblique Whistler-Mode Waves in the Earth's Inner Magnetosphere: Energy Distribution, Origins, and Role in Radiation Belt Dynamics. Space Sci. Rev. 200, 261–355. doi:doi:10.1007/s11214-016-0252-5.

[11] Artemyev, A.V., Mourenas, D., Agapitov, O.V., Vainchtein, D.L., Mozer, F.S., Krasnoselskikh, V.V., 2015a. Stability of relativistic electron trapping by strong whistler or electromagnetic ion cyclotron waves. Physics of Plasmas 22, 082901. doi:doi:10.1063/1.4927774.

[12] Artemyev, A.V., Neishtadt, A.I., Vainchtein, D.L., Vasiliev, A.A., Vasko, I.Y., Zelenyi, L.M., 2018a. Trapping (capture) into resonance and scattering on resonance: Summary of results for space plasma systems. Communications in Nonlinear Science and Numerical Simulations 65, 111–160. doi:doi:10.1016/j.cnsns.2018.05.004.

[13] Artemyev, A.V., Neishtadt, A.I., Vasiliev, A.A., Mourenas, D., 2018b. Long-term evolution of electron distribution function due to nonlinear resonant interaction with whistler mode waves. Journal of Plasma Physics 84, 905840206. doi:doi:10.1017/S0022377818000260.

[14] Artemyev, A.V., Vasiliev, A.A., Mourenas, D., Neishtadt, A.I., Agapitov, O.V., Krasnoselskikh, V., 2015b. Probability of relativistic electron trapping by parallel and oblique whistler-mode waves in Earth's radiation belts. Physics of Plasmas 22, 112903. doi:doi:10.1063/1.4935842.

[15] Bell, T.F., 1984. The nonlinear gyroresonance interaction between energetic electrons and coherent VLF waves propagating at an arbitrary angle with respect to the earth's magnetic field. J. Geophys. Res. 89, 905–918. doi:doi:10.1029/JA089iA02p00905.

[16] Cary, J.R., Escande, D.F., Tennyson, J.L., 1986. Adiabatic-invariant change due to separatrix crossing. Physical Review A 34, 4256–4275.

[17] Cattell, C., Wygant, J.R., Goetz, K., Kersten, K., Kellogg, P.J., von Rosenvinge, T., Bale, S.D., Roth, I., Temerin, M., Hudson, M.K., Mewaldt, R.A., Wiedenbeck, M., Maksimovic, M., Ergun, R., Acuna, M., Russell, C.T., 2008. Discovery of very large amplitude whistler-mode waves in Earth's radiation belts. Geophys. Res. Lett. 35, 1105. doi:doi:10.1029/2007GL032009.

[18] Demekhov, A.G., Trakhtengerts, V.Y., Rycroft, M., Nunn, D., 2009. Efficiency of electron acceleration in the Earth's magnetosphere by whistler mode waves. Geomagnetism and Aeronomy 49, 24–29. doi:doi:10.1134/S0016793209010034.

[19] Demekhov, A.G., Trakhtengerts, V.Y., Rycroft, M.J., Nunn, D., 2006. Electron acceleration in the magnetosphere by whistler-mode waves of varying frequency. Geomagnetism and Aeronomy 46, 711–716. doi:doi:10.1134/S0016793206060053.

[20] Drummond, W.E., Pines, D., 1962. Nonlinear stability of plasma oscillations. Nuclear Fusion Suppl. 3, 1049–1058.

[21] Fajans, J., Frièdland, L., 2001. Autoresonant (nonstationary) excitation of pendulums, Plutinos, plasmas, and other nonlinear oscillators. American Journal of Physics 69, 1096–1102. doi:doi:10.1119/1.1389278.

[22] Friedland, L., 2009. Autoresonance in nonlinear systems. Scholarpedia 4, 5473. doi:doi:10.4249/scholarpedia.5473.

[23] Furuya, N., Omura, Y., Summers, D., 2008. Relativistic turning acceleration of radiation belt electrons by whistler mode chorus. J. Geophys. Res. 113, 4224. doi:doi:10.1029/2007JA012478.

[24] Galeev, A.A., Sagdeev, R.Z., 1979. Nonlinear Plasma Theory, in: Leontovich, A.M.A. (Ed.), Reviews of Plasma Physics, Volume 7, p. 1.

[25] Gan, L., Li, W., Ma, Q., Albert, J.M., Artemyev, A.V., Bortnik, J., 2020. Nonlinear Interactions Between Radiation Belt Electrons and Chorus Waves: Dependence on Wave Amplitude Modulation. Geophys. Res. Lett. 47, e85987. doi:doi:10.1029/2019GL085987.

[26] Gary, S.P., Montgomery, D., Swift, D.W., 1968. Particle acceleration by electrostatic waves with spatially varying phase velocities. J. Geophys. Res. 73, 7524–7525. doi:doi:10.1029/JA073i023p07524.

[27] Grach, V.S., Demekhov, A.G., 2018a. Resonance Interaction of Relativistic Electrons with Ion-Cyclotron Waves. I. Specific Features of the Nonlinear Interaction Regimes. Radiophysics and Quantum Electronics 60, 942–959. doi:doi:10.1007/s11141-018-9860-0.

[28] Grach, V.S., Demekhov, A.G., 2018b. Resonant Interaction of Relativistic Electrons with Electromagnetic Ion-Cyclotron Waves. II. Integral Parameters of Interaction Regimes. Radiophysics and Quantum Electronics 61, 389–401. doi:doi:10.1007/s11141-018-9900-9.

[29] Grach, V.S., Demekhov, A.G., 2020. Precipitation of Relativistic Electrons Under Resonant Interaction With Electromagnetic Ion Cyclotron Wave Packets. Journal of Geophysical Research (Space Physics) 125, e27358. doi:doi:10.1029/2019JA027358.

[30] Henrard, J., Lemaitre, A., 1983. A Second Fundamental Model for Resonance. Celestial Mechanics 30, 197–218. doi:doi:10.1007/BF01234306.

[31] Hiraga, R., Omura, Y., 2020. Acceleration mechanism of radiation belt electrons through interaction with multi-subpacket chorus waves. Earth, Planets, and Space 72, 21. doi:doi:10.1186/s40623-020-1134-3.

[32] Hsieh, Y.K., Omura, Y., 2017. Nonlinear dynamics of electrons interacting with oblique whistler mode chorus in the magnetosphere. J. Geophys. Res. 122, 675–694. doi:doi:

10.1002/2016JA023255.

[33]Karpman, V.I., 1974. Nonlinear Effects in the ELF Waves Propagating along the Magnetic Field in the Magnetosphere. Space Sci. Rev. 16, 361–388. doi:doi:10.1007/BF00171564.

[34]Karpman, V.I., Istomin, I.N., Shkliar, D.R., 1975a. Effects of nonlinear interaction of monochromatic waves with resonant particles in the inhomogeneous plasma. Physica Scripta 11, 278–284. doi:doi:10.1088/0031-8949/11/5/008.

[35]Karpman, V.I., Istomin, J.N., Shklyar, D.R., 1974. Nonlinear theory of a quasi-monochromatic whistler mode packet in inhomogeneous plasma. Plasma Physics 16, 685–703. doi:doi:10.1088/0032-1028/16/8/001.

[36]Karpman, V.I., Istomin, J.N., Shklyar, D.R., 1975b. Particle acceleration by a non-linear langmuir wave in an inhomogeneous plasma. Physics Letters A 53, 101–102. doi:doi:10.1016/0375-9601(75)90364-3.

[37]Karpman, V.I., Shklyar, D.R., 1972. Nonlinear Damping of Potential Monochromatic Waves in an Inhomogeneous Plasma. Sov. JETP 35, 500.

[38]Katoh, Y., Omura, Y., 2007. Relativistic particle acceleration in the process of whistler-mode chorus wave generation. Geophys. Res. Lett. 34, L13102. doi:doi:10.1029/2007GL029758.

[39]Kennel, C.F., Petschek, H.E., 1966. Limit on Stably Trapped Particle Fluxes. J. Geophys. Res. 71, 1–28.

[40]Kitahara, M., Katoh, Y., 2019. Anomalous Trapping of Low Pitch Angle Electrons by Coherent Whistler Mode Waves. J. Geophys. Res. 124, 5568–5583. doi:doi:10.1029/2019JA026493.

[41]Kubota, Y., Omura, Y., 2017. Rapid precipitation of radiation belt electrons induced by EMIC rising tone emissions localized in longitude inside and outside the plasmapause. Journal of Geophysical Research (Space Physics) 122, 293–309. doi:doi:10.1002/2016JA023267.

[42]Kubota, Y., Omura, Y., 2018. Nonlinear Dynamics of Radiation Belt Electrons Interacting With Chorus Emissions Localized in Longitude. Journal of Geophysical Research (Space Physics) 123, 4835–4857. doi:doi:10.1029/2017JA025050.

[43]Landau, L.D., Lifshitz, E.M., 1960. Vol. 1: Mechanics. Course of Theoretical Physics. 1st ed., Oxford: Pergamon Press.

[44]Laval, G., Pellat, R., 1970. Particle acceleration by electrostatic waves propagating in an inhomogeneous plasma. J. Geophys. Res. 75, 3255–3256. doi:doi:10.1029/JA075i016p03255.

[45]Le Queau, D., Roux, A., 1987. Quasi-monochromatic wave-particle interactions in magnetospheric plasmas. Solar Physics 111, 59–80. doi:doi:10.1007/BF00145441.

[46]Li, W., Hudson, M.K., 2019. Earth's Van Allen Radiation Belts: From Discovery to the Van Allen Probes Era. Journal of Geophysical Research (Space Physics) 124, 8319–8351. doi:doi:10.1029/2018JA025940.

[47]Lundin, B.V., Shkliar, D.R., 1977. Interaction of electrons with low transverse velocities with VLF waves in an inhomogeneous plasma. Geomagnetism and Aeronomy 17, 246–251.

[48]Millan, R.M., Thorne, R.M., 2007. Review of radiation belt relativistic electron losses. Journal of Atmospheric and Solar-Terrestrial Physics 69, 362–377. doi:doi:10.1016/j.jastp.2006.06.019.

[49]Mourenas, D., Zhang, X.J., Artemyev, A.V., Angelopoulos, V., Thorne, R.M., Bortnik, J., Neishtadt, A.I., Vasiliev, A.A., 2018. Electron Nonlinear Resonant Interaction With Short and Intense Parallel Chorus Wave Packets. J. Geophys. Res. 123, 4979–4999. doi:doi:10.1029/2018JA025417.

[50]Neishtadt, A., 1975. Passage through a separatrix in a resonance problem with a slowly-varying parameter. Journal of Applied Mathematics and Mechanics 39, 594–605. doi:doi:10.1016/0021-8928(75)90060-X.

[51]Neishtadt, A., 1981. On the accuracy of conservation of the adiabatic invariant. Journal of Applied Mathematics and Mechanics 45, 58–63. doi:doi:10.1016/0021-8928(81)90010-1.

[52]Neishtadt, A., 1987. On the change in the adiabatic invariant on crossing a separatrix in systems with two degrees of freedom. Journal of Applied Mathematics and Mechanics 51, 586–592. doi:doi:10.1016/0021-8928(87)90006-2.

[53]Neishtadt, A., 2019. On mechanisms of destruction of adiabatic invariance in slow-fast hamiltonian systems. Nonlinearity 32, R53–R76. URL: `https://doi.org/10.1088%2F1361-6544%2Fab2a2c`, doi:doi:10.1088/1361-6544/ab2a2c.

[54]Neishtadt, A.I., 1986. Change of an adiabatic invariant at a separatrix. Soviet Journal of Plasma Physics 12, 568–573.

[55]Neishtadt, A.I., 2014. Averaging, passage through resonances, and capture into resonance in two-frequency systems. Russian Mathematical Surveys 69, 771. URL: `http://stacks.iop.org/0036-0279/69/i=5/a=771`.

[56]Neishtadt, A.I., Petrovichev, B.A., Chernikov, A.A., 1989. Particle entrainment into unlimited acceleration. Soviet Journal of Plasma Physics 15, 1021–1023.

[57]Neishtadt, A.I., Vasiliev, A.A., Artemyev, A.V., 2013. Capture into resonance and escape from it in a forced nonlinear pendulum. Regular and Chaotic Dynamics 18, 686–696. doi:doi:10.1134/S1560354713060087, `arXiv:1309.6501`.

[58]Nunn, D., 1971. Wave-particle interactions in electrostatic waves in an inhomogeneous medium. Journal of Plasma Physics 6, 291. doi:doi:10.1017/S0022377800006061.

[59]Nunn, D., 1974. A self-consistent theory of triggered VLF emissions. Plan. Sp. Sci. 22, 349–378. doi:doi:10.1016/0032-0633(74)90070-1.

[60]Nunn, D., 1986. A nonlinear theory of sideband stability in ducted whistler mode waves. Plan. Sp. Sci. 34, 429–451. doi:doi:10.1016/0032-0633(86)90032-2.

[61]Nunn, D., Omura, Y., 2015. A computational and theoretical investigation of nonlinear wave-particle interactions in oblique whistlers. J. Geophys. Res. 120, 2890–2911. doi:doi:10.1002/2014JA020898.

[62]Omura, Y., Furuya, N., Summers, D., 2007. Relativistic turning acceleration of resonant electrons by coherent whistler mode waves in a dipole magnetic field. J. Geophys. Res. 112, 6236. doi:doi:10.1029/2006JA012243.

[63]Omura, Y., Matsumoto, H., Nunn, D., Rycroft, M.J., 1991. A review of observational, theoretical and numerical studies of VLF triggered emissions. Journal of Atmospheric and Terrestrial Physics 53, 351–368.

[64]Shapiro, V.D., Sagdeev, R.Z., 1997. Nonlinear wave-particle interaction and conditions for the applicability of quasilinear theory. Physics Reports 283, 49–71. doi:doi:10.1016/S0370-1573(96)00053-1.

[65]Shklyar, D.R., 1981. Stochastic motion of relativistic particles in the field of a monochromatic wave. Sov. Phys. JETP 53, 1197–1192.

[66]Shklyar, D.R., Matsumoto, H., 2009. Oblique Whistler-Mode Waves in the Inhomogeneous Magnetospheric Plasma: Resonant Interactions with Energetic Charged Particles. Surveys in Geophysics 30, 55–104. doi:doi:10.1007/s10712-009-9061-7.

[67]Solovev, V.V., Shkliar, D.R., 1986. Particle heating by a low-amplitude wave in an inhomogeneous magnetoplasma. Sov. Phys. JETP 63, 272–277.

[68]Stix, T.H., 1962. The Theory of Plasma Waves.

[69]Summers, D., Omura, Y., 2007. Ultra-relativistic acceleration of electrons in planetary magnetospheres. Geophys. Res. Lett. 34, 24205. doi:doi:10.1029/2007GL032226.

[70]Tao, X., Bortnik, J., 2010. Nonlinear interactions between relativistic radiation belt electrons and oblique whistler mode waves. Nonlinear Processes in Geophysics 17, 599–604. doi:doi:10.5194/npg-17-599-2010.

[71]Tao, X., Bortnik, J., Albert, J.M., Liu, K., Thorne, R.M., 2011. Comparison of quasilinear diffusion coefficients for parallel propagating whistler mode waves with test particle simulations. Geophys. Res. Lett. 38, 6105. doi:doi:10.1029/2011GL046787.

[72]Tao, X., Bortnik, J., Albert, J.M., Thorne, R.M., Li, W., 2013. The importance of amplitude modulation in nonlinear interactions between electrons and large amplitude whistler waves. Journal of Atmospheric and Solar-Terrestrial Physics 99, 67–72. doi:doi:10.1016/j.jastp.2012.05.012.

[73]Thorne, R.M., 2010. Radiation belt dynamics: The importance of wave-particle interactions. Geophys. Res. Lett. 372, 22107. doi:doi:10.1029/2010GL044990.

[74]Tyler, E., Breneman, A., Cattell, C., Wygant, J., Thaller, S., Malaspina, D., 2019. Statistical Occurrence and Distribution of High-Amplitude Whistler Mode Waves in the Outer Radiation Belt. Geophys. Res. Lett. 46, 2328–2336. doi:doi:10.1029/2019GL082292.

[75]Vainchtein, D., Zhang, X.J., Artemyev, A., Mourenas, D., Angelopoulos, V., Thorne, R.M., 2018. Evolution of electron distribution driven by nonlinear resonances with intense field-aligned chorus waves. J. Geophys. Res. doi:doi:10.1029/2018ja025654.

[76]Vedenov, A.A., Sagdeev, R.Z., 1961. Some properties of a plasma with an anisotropic ion velocity distribution in a magnetic field, in: Leontovich, M.A. (Ed.), Plasma Physics and the Problem of Controlled Thermonuclear Reactions, Volume 3, p. 332.

[77]Vedenov, A.A., Velikhov, E., Sagdeev, R., 1962. Quasilinear theory of plasma oscillations. Nuclear Fusion Suppl. 2, 465–475.

[78]Wilson, III, L.B., Cattell, C.A., Kellogg, P.J., Wygant, J.R., Goetz, K., Breneman, A., Kersten, K., 2011. The properties of large amplitude whistler mode waves in the magnetosphere: Propagation and relationship with geomagnetic activity. Geophys. Res. Lett. 38, 17107. doi:doi:10.1029/2011GL048671.

[79]Zhang, X.J., Mourenas, D., Artemyev, A.V., Angelopoulos, V., Bortnik, J., Thorne, R.M., Kurth, W.S., Kletzing, C.A., Hospodarsky, G.B., 2019. Nonlinear Electron Interaction With Intense Chorus Waves: Statistics of Occurrence Rates. Geophys. Res. Lett. 46, 7182–7190. doi:doi:10.1029/2019GL083833.

[80]Zhang, X.J., Mourenas, D., Artemyev, A.V., Angelopoulos, V., Kurth, W.S., Kletzing, C.A., Hospodarsky, G.B., 2020. Rapid Frequency Variations Within Intense Chorus Wave Packets. Geophys. Res. Lett. 47, e88853. doi:doi:10.1029/2020GL088853.

[81]Zhang, X.J., Thorne, R., Artemyev, A., Mourenas, D., Angelopoulos, V., Bortnik, J., Kletzing, C.A., Kurth, W.S., Hospodarsky, G.B., 2018. Properties of intense field-aligned lower-band chorus waves: Implications for nonlinear wave-particle interactions. J. Geophys. Res. 123, 5379–5393. URL: https://agupubs.onlinelibrary.wiley.com/doi/abs/10.1029/2018JA025390, doi:doi:10.1029/2018JA025390, arXiv:https://agupubs.onlinelibrary.wiley.com/doi/pdf/10.1029/2018JA